Structure
Short Article

Molecular Organization and ATP-Induced Conformational Changes of ABCA4, the Photoreceptor-Specific ABC Transporter

Yaroslav Tsybovsky,[1,*] Tivadar Orban,[1] Robert S. Molday,[2] Derek Taylor,[1] and Krzysztof Palczewski[1,*]
[1]Department of Pharmacology, School of Medicine, Case Western Reserve University, Cleveland, OH 44106, USA
[2]Department of Biochemistry and Molecular Biology, Centre for Macular Research, University of British Columbia, Vancouver, BC V6T 1Z3, Canada
*Correspondence: yxt76@case.edu (Y.T.), kxp65@cwru.edu (K.P.)
http://dx.doi.org/10.1016/j.str.2013.03.001

SUMMARY

ATP-binding cassette (ABC) transporters use ATP to translocate various substrates across cellular membranes. Several members of subfamily A of mammalian ABC transporters are associated with severe health disorders, but their unusual complexity and large size have so far precluded structural characterization. ABCA4 is localized to the discs of vertebrate photoreceptor outer segments. This protein transports *N*-retinylidene-phosphatidylethanolamine to the outer side of disc membranes to prevent formation of toxic compounds causing macular degeneration. An 18 Å-resolution structure of ABCA4 isolated from bovine rod outer segments was determined using electron microscopy and single-particle reconstruction. Significant conformational changes in the cytoplasmic and transmembrane regions were observed upon binding of a nonhydrolyzable ATP analog and accompanied by altered hydrogen/deuterium exchange in the Walker A motif of one of the nucleotide-binding domains. These findings provide an initial view of the molecular organization and functional rearrangements for any member of the ABCA subfamily of ABC transporters.

INTRODUCTION

ATP-binding cassette (ABC) transporters are an ancient superfamily of integral membrane proteins that serve a general purpose of selective transport across biological membranes. Widely distributed throughout all domains of life, they use the energy of ATP hydrolysis to import or expel a great variety of substances, ranging from inorganic ions to polypeptides (Higgins, 1992; Holland and Blight, 1999). These proteins share a common core architecture, comprised of two transmembrane domains (TMDs) and two nucleotide-binding domains (NBDs), also known as ATP-binding cassettes. Evolutionary divergence within the superfamily has resulted in altered modes of structural organization of these four components (Higgins, 1992). In prokaryotes, they are usually produced as separate proteins or TMD-NBD tandems, which associate to form a functional transporter, whereas in eukaryotes, they often reside within a single polypeptide chain (Kos and Ford, 2009). The broad distribution and substrate diversity of ABC transporters are further reflected in low amino acid sequence similarity among them, with the exception of highly conserved NBDs.

Based on gene organization and sequence analysis, mammalian ABC transporters are divided into seven subfamilies: ABCA through ABCG (Vasiliou et al., 2009). The human ABCA subfamily is composed of 12 members that are likely involved in lipid transport (Piehler et al., 2012). This subfamily contains unusually large and complex proteins, such as ABCA13, which is comprised of more than 5,000 residues. Accordingly, ABCA transporters significantly deviate from the minimal four-domain architecture described above. A distinctive topological element of these proteins is the large N-terminal extracellular domain of poorly defined function, whereas the cytosolic domains extend beyond the consensus NBD sequence. Despite considerable effort, molecular level studies of the members of the A subfamily have been limited. In particular, low abundance and high complexity have so far precluded structural characterization of ABCA transporters.

ABCA4, a member of the ABCA subfamily, is predominantly expressed in the outer segments of rod and cone photoreceptors, where it is found in rims and incisures of disk membranes (Molday et al., 2000; Papermaster et al., 1978, 1982; Sun and Nathans, 1997). The main role of ABCA4 is in clearance of all-*trans*-retinal (ATR), the product of light-induced isomerization of the visual pigment chromophore, 11-*cis*-retinal, from photoreceptors (Ahn et al., 2000; Maeda et al., 2008; Sun et al., 1999; Weng et al., 1999). More specifically, ABCA4 transports *N*-retinylidene-phosphatidylethanolamine (*N*-retinylidene-PE) from the luminal to the cytoplasmic (CT) side of the disk membrane, thereby preventing formation of toxic condensation products (Quazi et al., 2012). Mutations in the *ABCA4* gene have been linked to devastating visual disorders, such as Stargardt disease, an early onset macular degeneration (Allikmets et al., 1997a; Weleber, 1994), retinitis pigmentosa (Martínez-Mir et al., 1998), cone-rod dystrophy (Hamel, 2007) and a higher susceptibility to develop age-related macular degeneration (Allikmets et al., 1997b).

ABCA4 is a single-chain protein with 2,273 residues (human ortholog) organized in two homologous but not identical parts, each carrying a TMD with six predicted membrane-spanning

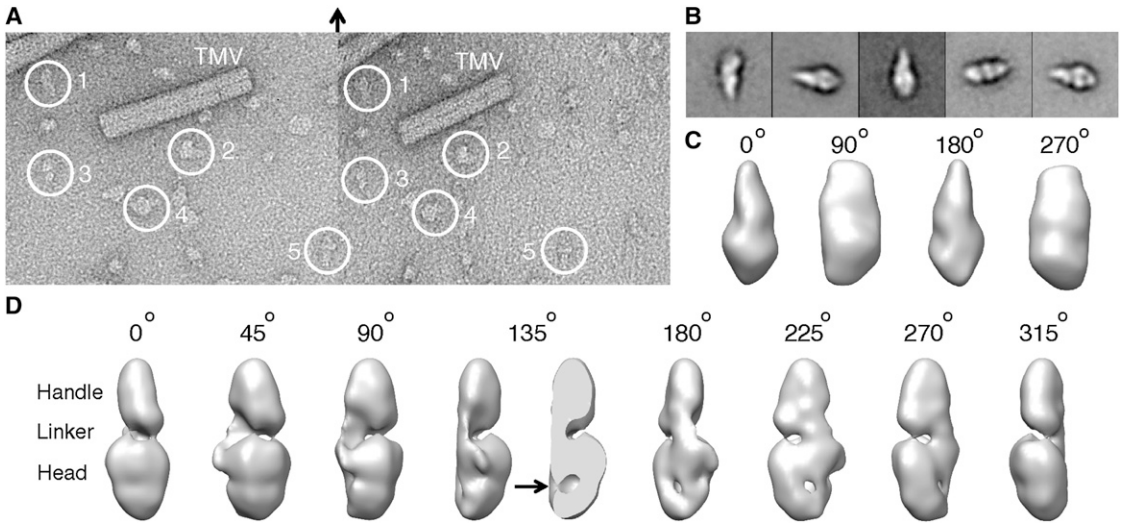

Figure 1. Structure of ABCA4 Determined by EM

(A) Untilted (left) and 45° tilted (right) EM micrographs of uranyl acetate-stained ABCA4. The tilt axis is marked with an arrow. Examples of ABCA4 particles forming tilt pairs are enclosed in circles and marked with numbers. TMV, tobacco mosaic virus.

(B) Examples of 2D class averages generated using untilted particles.

(C) Angular views of the RCT model of ABCA4.

(D) Angular views of the final ABCA4 structure filtered to 19 Å resolution. A cross-section with the exposed internal cavity (marked with an arrow) is shown for the 135° view.

See also Figure S1.

helices, an exocytoplasmic (intradiscal [ID]) domain (ECD), and a cytoplasmic domain (CD) that hosts an NBD. This topology was supported by multiple glycosylation sites identified in ECDs, whereas CD1 was found to be phosphorylated (Bungert et al., 2001; Tsybovsky et al., 2011).

Here, we present a structural study of ABCA4. Our ligand-free and ATP-bound structures obtained by electron microscopy (EM) and single-particle reconstruction reveal the molecular architecture of bovine ABCA4 and illustrate the conformational transitions that result from nucleotide binding. Complementary hydrogen/deuterium (H/D) exchange studies demonstrate ATP-induced alterations in the local environment of the Walker A motif and suggest that only one NBD is catalytically active. This work provides direct structural information and mechanistic insights into the function of ABCA4.

RESULTS

Isolation and Biochemical Characterization of ABCA4

We developed an isolation procedure that allows purification of ABCA4 from a native source, rod outer segments (ROS) of bovine photoreceptors, in quantities sufficient for structural analysis (see Supplemental Experimental Procedures; Figure S1A available online). This protocol yields 0.1–0.3 mg of highly purified ABCA4 from 100 bovine retinas. Immediately after purification, the detergent bound to ABCA4 was replaced with Amphipol A8-35 (Amphipol) (Popot et al., 2011), resulting in formation of a monodisperse ABCA4-Amphipol complex and removing the need to maintain excess detergent or Amphipol in solution. When subjected to size exclusion chromatography, ABCA4 eluted in a single symmetrical peak with an apparent molecular weight (MW) of about 400 kDa (Figure S1B), corresponding well to a theoretical value of 360 kDa calculated for a complex comprising one molecule of ABCA4 (260 kDa plus ~20 kDa to account for glycosylation; Tsybovsky et al., 2011) and approximately 80 kDa of Amphipol needed to cover 12 transmembrane (TM) helices. This Amphipol amount was estimated based on the Amphipol:protein ratio determined for bacteriorhodopsin (Gohon et al., 2008). In our experiments, the basal ATPase activity of ABCA4 in the presence of Amphipol was consistently higher than that of the detergent-solubilized protein (Figure S1C), which may reflect the stabilizing effect of Amphipol. Addition of 1 mM adenosine 5′-(β,γ-imido) triphosphate (AMPPNP), a nonhydrolyzable ATP analog, substantially inhibited the ATPase activity.

Molecular Architecture of ABCA4

We used negative-stain EM and single-particle analysis to determine the structure of ABCA4. An initial three-dimensional (3D) map obtained with the random conical tilt (RCT) method (Figures 1A–1C) was improved with reference-based angular refinement (Figures S1D–S1F). The final 18.1 Å-resolution structure of ABCA4 revealed a complex elongated asymmetrical shape that measured 20 nm in its longest dimension (Figure 1D). The molecule resembles an upside-down ice cream cone with a "handle" and "head" connected by a thinner linker region. The head portion featured a solvent-exposed internal cavity with a diameter of roughly 3 nm (Figure 1D).

In the absence of structural information regarding members of the ABCA subfamily of ABC transporters, we took advantage of the fact that ECD1 and ECD2 of ABCA4 are glycosylated at seven different sites (Tsybovsky et al., 2011; Figure 2A) to

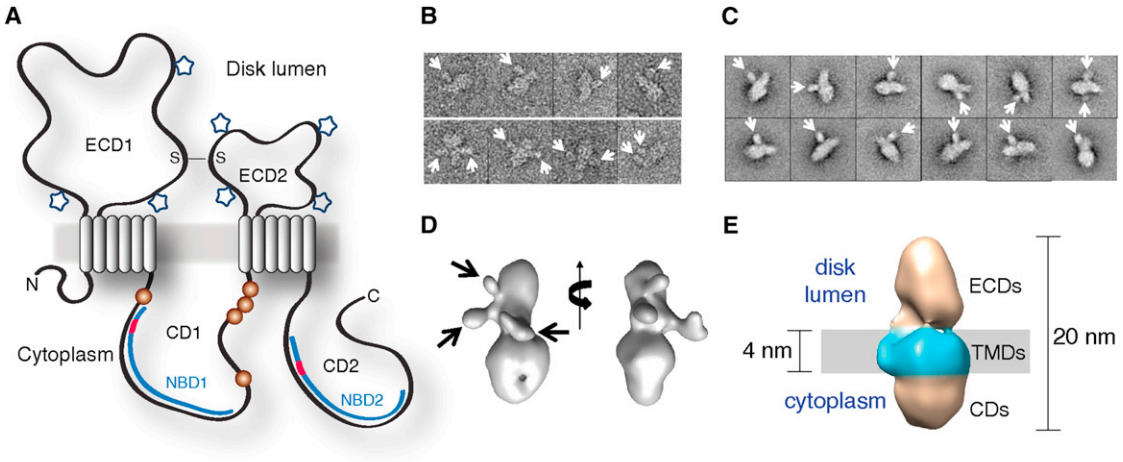

Figure 2. Identification of Intradiscal Regions of ABCA4

(A) A topological model of ABCA4 based on published evidence (Bungert et al., 2001; Tsybovsky et al., 2011). ATP-binding Walker A motifs located in NBDs are colored red. Glycosylation sites are shown with stars and phosphorylation sites with brown spheres. A disulfide bridge between ECD1 and ECD2 (Bungert et al., 2001) is marked S-S.

(B) Examples of ABCA4 particles with one (top row) or two (bottom row) bound molecules of succinylated ConA (53 kDa in size). ConA particles are marked with white arrows.

(C) Examples of 2D class averages of the ABCA4-ConA complex. ConA molecules bound exclusively to the handle and linker regions of ABCA4, identifying them as ECDs.

(D) A 3D reconstruction of the ABCA4-ConA complex, illustrating positions of three ConA binding sites (black arrows).

(E) The EM model of ABCA4 with assigned ECDs, TMDs, and CDs. The proposed Amphipol belt around the TM region is colored in cyan. Grey rectangle represents the anticipated position of the lipid bilayer.

See also Figure S2.

identify their positions in the structure. Screening of lectins revealed that Concanavalin A (ConA) is capable of strongly binding to ABCA4 glycans. Therefore, an ABCA4-ConA complex was assembled by incubation of ABCA4 with succinylated ConA and subjected to negative staining and EM analysis. Visual examination of 5,196 ABCA4 particles revealed that 2,123 of them had additional density consistent with the 53 kDa MW of succinylated ConA. We observed complexes composed of one molecule of ABCA4 bound to one (81% of particles) or two (19% of particles) molecules of ConA (Figure 2B). Reference-free alignment and classification revealed pronounced ConA density attached to various sites on ABCA4 (Figure 2C). This density was strong in most of the two-dimensional (2D) classes but less ordered in some others, presumably because of the conformational flexibility of the polysaccharides decorating ABCA4. ConA bound exclusively to the handle and linker regions (Figures 2B and 2C), thus identifying them as the ID portion composed of glycosylated ECD1 and ECD2. To more precisely identify the binding regions, we determined a 3D map of the ABCA4-ConA complex (Figure 2D). This map revealed three primary sites for ConA binding, all of them in the handle and linker regions. By exclusion, the head of the molecule should contain the TMDs and CDs.

Further assignment of CDs and TMDs within the head of the molecule can be suggested based on the above results and the proposed ABCA4 topology (Figure 2A). The ID and CT moieties of ABCA4 are similar in molecular weight (on the order of 100 kDa each), which implies a central position of the TM region. In agreement with this, an elevated zone spanning the circumference of the EM model was observed in the head portion of the molecule adjacent to the ID region (Figure 2E). The height of this zone was equal to that estimated for the Amphipol belt (4 nm) (Althoff et al., 2011). Furthermore, when the horizontal cross-section of the map in the center of the suggested TM region was analyzed and an estimated 2-nm-thick layer was subtracted for Amphipol belt (Althoff et al., 2011), this left a remaining central area of 16.5 nm^2 (Figure S2). This area corresponds well with the sectional area of twelve TM helices (16.8 nm^2), assuming a 1.4 nm^2 sectional area of a single helix (Eskandari et al., 1998). Based on these considerations, it can also be inferred that CDs occupy the bottom part of the head region.

Conformational Changes Associated with Binding of AMPPNP

The structure of ABCA4 in the presence of AMPPNP/Mg^{2+}, determined by using the nucleotide-free map as the initial reference, showed significant alterations (Figure 3A). Binding of this nonhydrolyzable ATP analog led to a constriction of the internal cavity in the CT region of the molecule, as well as to the loss of connectivity between this cavity and the surface (Figure 3B; Movie S1). The overall shape change visible in the CT portion of the protein propagated into the TM region (Figure 3B; Movie S1). The combined change in the appearance of the CT and TM regions can be described as tightening of the head moiety. The significance of the observed changes was validated by determining the ligand-free and AMPPNP-bound structures with different starting models used for reference-based reconstruction and refinement (see Figure S3 and associated text in

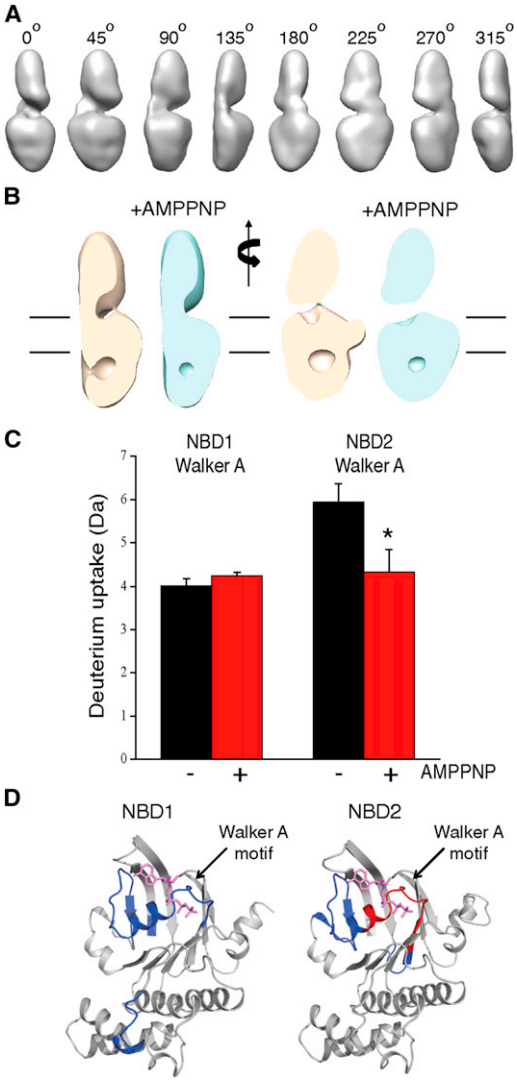

Figure 3. Global and Local Conformational Changes in ABCA4 Induced by Binding of AMPPNP

(A) Angular views of the ABCA4 structure determined in the presence of AMPPNP. The structure was filtered to 19 Å resolution.

(B) Views of ligand-free (tan) and AMPPNP-bound (light blue) EM maps of ABCA4 with the front surface cut away to expose the internal cavity. Lines indicate the suggested position of the membrane.

(C) Deuterium uptake by the Walker A ATP-binding motif of NBD1 (left) and NBD2 (right) in the absence (black) and presence (red) of AMPPNP. Addition of AMPPNP decreased the uptake in NBD2 but not NBD1. Data are represented as mean ± SD. The statistically significant difference ($p = 5.5 \times 10^{-7}$) is marked with an asterisk.

(D) In silico models of NBD1 (left) and NBD2 (right) with peptides showing no changes versus significant changes in deuterium uptake upon addition of AMPPNP shown in blue and red, respectively. ATP molecules (pink) were positioned for illustration purposes based on the superimposed crystal structure of a homologous NBD domain (Protein Data Bank code 3FVQ).

See also Figure S3, Movie S1, and Table S1.

Supplemental Information). In contrast, no structural alterations were detected in the ID region of ABCA4 upon AMPPNP binding.

Local Environment of the ATP-Binding Sites

Application of H/D exchange coupled with mass spectrometry to membrane proteins remains a challenging task, with the first study of a 63 kDa prokaryotic ABC transporter BmrA published only recently (Mehmood et al., 2012). We achieved peptide sequence coverage of 34% for Amphipol-embedded ABCA4 digested with pepsin. The number of peptides suitable for analysis (Table S1) was further reduced, owing to the deuteration-induced isotopic envelope widening. Nevertheless, peptides forming ATP-binding Walker A motifs (LGHNGAGKTTTL in NBD1 and FGLLGVNGAGKTTTF in NBD2) were reliably detected. Quantification of the H/D exchange in these areas showed a radically different behavior of NBD1 versus NBD2 (Figure S3D). Addition of AMPPNP reduced the H/D exchange in the peptide carrying the Walker A motif of NBD2 by about 30% (Figures 3C and S3D), indicating a substantial change in its local environment (Figure 3D). In contrast, no statistically significant changes were found in the equivalent region of NBD1 ($p > 0.05$). Peptides adjacent to Walker A motifs did not manifest ATP-induced changes in either of the NBDs (Figure 3D; Table S1). Thus, H/D exchange studies confirmed the structural alterations in the CT region of ABCA4 revealed by the EM structures.

DISCUSSION

Being among the largest proteins of the superfamily, ABCA4 is unique in that it is the only mammalian ABC transporter shown to function as an importer (Quazi et al., 2012). Predominant localization in photoreceptors, which can be readily separated from other retinal cells, offers a rare opportunity to obtain this member of the ABCA subfamily directly from the native source, thereby avoiding a spectrum of complications associated with recombinant expression of large membrane proteins. We developed an efficient and scalable purification procedure that allowed isolating bovine ABCA4 from membranes of ROS (Figure S1A). Additionally, using Amphipol instead of detergent led to monodisperse ABCA4 preparations with preserved basal ATPase activity, which permitted analysis by transmission EM and single particle reconstruction.

Biochemical and computational evidence predicts an ornate topology of ABCA4 comprised of two CDs, two unusually large (a total of ~900 residues) exocytoplasmic loops located inside the rim of the disc, and 12 TM helices (Bungert et al., 2001; Peelman et al., 2003; Tsybovsky et al., 2011; Figure 2A). Our EM analysis of ABCA4 revealed that the ID portion of the protein, which constitutes the hallmark of the ABCA subfamily, is well ordered and tightly packed in a single structural unit that protrudes about 10 nm deep into the rim space (Figure S4). This geometry can explain the strict localization of ABCA4 to the rims of rod discs (Illing et al., 1997), as the reported ID space outside of rims (3–5 nm) (Nickell et al., 2007) is insufficient to accommodate the ECDs. The biological role of ECDs is currently unclear. It has been suggested that ECDs of ABCA1 are responsible for interactions with apolipoprotein A-1 (Fitzgerald et al., 2002), whereas recombinantly expressed ECD2 of ABCA4 might interact with ATR (Biswas-Fiss et al., 2010). Additional studies will be necessary to define the function of ECDs.

Despite the existence of a solvent-exposed internal cavity in the CT region of the protein, the two CDs also form a combined

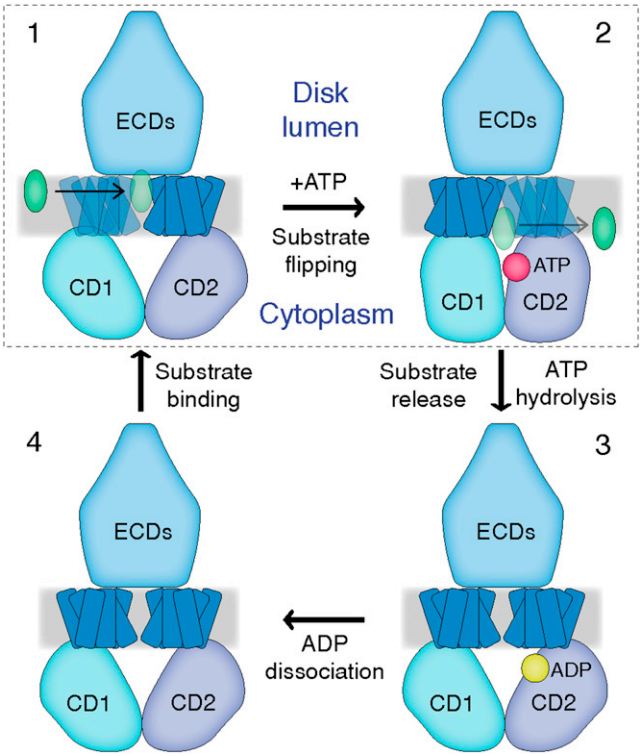

Figure 4. A Hypothetical Model of ABCA4 Transport Composed of Four Principle Stages

N-retinylidene-PE is shown as a green oval, whereas ATP and ADP are represented with red and yellow circles, respectively. The TM region is colored dark blue. Binding of ATP by NBD2 (stage 2) induces a tighter contact between the CDs, which is associated with rearrangements in the TM region that leads to substrate translocation. The rectangle encompasses the two stages of the transport cycle visualized in this study, assuming that binding of *N*-retinylidene-PE by itself does not induce global conformational changes.
See also Figure S4.

entity (Figures 1D and 3A). It is known that dimerization of NBDs is necessary for ATP hydrolysis (George and Jones, 2012). Our results agree well with X-ray and EM studies arguing that cytosolic domains of ABC transporters remain in contact, even in the absence of ATP (Hohl et al., 2012; Lee et al., 2002), as opposed to other crystal structures that suggest their complete separation in the resting state by as much as 20–30 Å (Aller et al., 2009; Ward et al., 2007). At the current resolution, however, a substantially smaller gap between the NBDs cannot be excluded. Intense interactions between the N- and C-terminal halves of ABCA4 are supported by the loss of both the basal and retinal-stimulated ATPase activities when they were expressed as separate proteins (Ahn et al., 2003). The sectional area of the TM region enclosed in the Amphipol belt is in good agreement with the presence of 12 membrane-spanning helices. Of note, with the exception of highly conserved NBDs, members of the ABCA subfamily show little to no sequence homology to other proteins. Within the subfamily, however, this homology is significant, with the sequence identity between ABCA1 and ABCA4 reaching 51%. It is thus reasonable to expect that other ABCA transporters have a similar molecular architecture.

Our data revealed ATP-induced structural rearrangements in ABCA4 manifested as a reduced volume of the internal cavity and an altered shape of the head of the molecule, where the CT and TM regions are likely to reside (Figure 3B; Movie S1). Such a constriction of the internal cavity may reflect a rearrangement or dimerization of NBDs and/or a general stabilization and loss of flexibility in the region involved in ATP binding and hydrolysis. The two hypotheses describing the mechanism of action of ABC transporters, the ATP switch model (Higgins and Linton, 2004), and the constant contact model (Jones and George, 2009) disagree with respect to the magnitude of changes that take place in the intracellular region during the transport cycle, but they agree that such changes are necessary. Although reliable docking of homology models of NBDs into our EM structures is not possible, given that NBDs constitute less than 50% of the intracellular portion of ABCA4, location of NBDs in the vicinity of the internal cavity can be inferred from the positions of the TM and CT moieties in the head of the molecule (Figure 2E). At the current resolution of 18 to 19 Å, however, it cannot be excluded that the observed changes are due to rearrangements of other portions of CDs. On the other hand, we see clear evidence that nucleotide binding results in the ''tightening'' of the CT moiety, as revealed by our EM and H/D exchange analysis, which agrees well with a lower level of conformational dynamics in the intracellular domains of the BmrA ABC transporter in the presence of ATP (Mehmood et al., 2012). Remarkably, constriction of the cavity is associated with structural changes in the TM region (Figure 3B; Movie S1), suggesting that binding of AMPPNP is coupled to a conformational transition in the membrane-spanning helices. Coupling of ATP binding and hydrolysis to structural rearrangements in TMDs, which allows active transport of the substrate through the lipid bilayer, constitutes the essence of the functional mechanism of ABC transporters (George and Jones, 2012; Higgins and Linton, 2004).

We propose that the global conformational changes in response to binding of AMPPNP revealed by EM are associated with an altered local environment of the consensus Walker A motif in NBD2 (Figures 3C and 3D). Our H/D exchange experiments showed that the Walker A motif of NBD2 is more protected in ATP-bound state, while exchange in the same region in NBD1 was not altered by the addition of AMPPNP. This may suggest that NBD1 either does not bind ATP or already has a bound nucleotide. The second explanation is in line with the conclusions of a previous biochemical study, which showed that NBD1 cannot be labeled with 8-azido-ATP and that a tightly bound ADP molecule can be extracted from ABCA4 after protein denaturation (Ahn et al., 2003). Similarly, atypical NBDs that are not capable of ATP hydrolysis but have a stably bound ATP molecule were described for ABCC7 (Aleksandrov et al., 2002) and the TM287/288 ABC transporter from *Thermotoga maritima* (Hohl et al., 2012). Such inactive NBDs can still play an important role in nucleotide hydrolysis by providing an ATP-binding interface and orchestrating catalysis through interactions with their catalytically active partners.

Combined with the accumulated body of biochemical evidence, our study suggests a transport model (Figure 4), in which, in the resting state, TMDs of ABCA4 form a conformation that is ready to accept *N*-retinylidene-PE from the luminal side of the disc membrane. It was shown that ABCA4 can recruit

N-retinylidene-PE in the absence of ATP (Beharry et al., 2004). In the next step, binding of a nucleotide by NBD2 initiates conformational changes in the tightly interacting CDs, which propagate to the TM region, leading to flipping of the substrate to the CT face of the membrane. The substrate can dissociate at this point or, as suggested by a higher efficiency of *N*-retinylidene-PE release by ATP compared to AMPPNP (Beharry et al., 2004), this dissociation could be facilitated by or depend on nucleotide hydrolysis. Finally, hydrolysis of ATP by NBD2 followed by dissociation of ADP restores the resting state of ABCA4.

In conclusion, we provide the initial view of the molecular organization and transport-related conformational transitions of ABCA4, an ABC transporter implicated in recycling of harmful byproducts of the visual cycle. These results lay a foundation for structural studies of the ABCA subfamily of human ABC transporters.

EXPERIMENTAL PROCEDURES

Full Experimental Procedures can be found in the Supplemental Information.

Purification of ABCA4 from Bovine ROS

ABCA4 was purified from detergent-solubilized ROS membranes in three consecutive steps, including ion exchange chromatography on DE52 resin, ligand affinity chromatography on Mimetic Red3 resin, and lectin affinity chromatography on *Galanthus nivalis* lectin (GNL) agarose. The resulting sample was incubated with 0.2 mg/ml Amphipol A8-35, concentrated and subjected to size exclusion chromatography on a Superose 6 column. For structural studies of the ABCA4-AMPPNP complex, purified ABCA4 was incubated with 2 mM $MgCl_2$ and 1 mM AMPPNP at 4°C overnight.

Transmission EM and Single-Particle Reconstruction

ABCA4 from peak Superose 6 fractions was adsorbed onto carbon-coated, glow-discharged EM grids and stained with 1% (w/v) uranyl acetate. Data were collected with a FEI Tecnai F20 microscope (FEI, Eindhoven, The Netherlands) operated at 200 kV. The initial 3D model of ligand-free ABCA4 was obtained by the RCT method (Radermacher et al., 1987). This model was used as the reference for the referenced-based projection alignment (Shaikh et al., 2008). The 3D structure of the ABCA4-AMPPNP complex was determined using the same referenced-based projection alignment protocol, with the final ligand-free ABCA4 or the RCT models as initial references.

ACCESSION NUMBERS

The EMDataBank accession numbers for the structures of ligand-free ABCA4 and the ABCA4-AMPPNP complex reported in this paper are EMD-5497 and EMD-5498, respectively.

SUPPLEMENTAL INFORMATION

Supplemental Information includes four figures, one movie, one table, and Supplemental Experimental Procedures and can be found with this article online at http://dx.doi.org/10.1016/j.str.2013.03.001.

ACKNOWLEDGMENTS

We are grateful to Dr. Andreas Engel and Dr. Vera Moiseenkova-Bell for helpful discussions and to Dr. Leslie T. Webster, Jr., and Dr. Phoebe Stewart for critical comments on the manuscript. We also thank Heather Holdaway for technical assistance. This research was supported, in whole or in part, by EY009339 (to K.P.), EY021126 (to K.P.), and EY002422 (to R.S.M.), grants from National Institutes of Health. K.P. is a John H. Hord Professor of Pharmacology, and R.S.M. is a Canada Research Chair in vision and macular degeneration.

Received: December 1, 2012
Revised: February 4, 2013
Accepted: March 1, 2013
Published: April 4, 2013

REFERENCES

Ahn, J., Wong, J.T., and Molday, R.S. (2000). The effect of lipid environment and retinoids on the ATPase activity of ABCR, the photoreceptor ABC transporter responsible for Stargardt macular dystrophy. J. Biol. Chem. *275*, 20399–20405.

Ahn, J., Beharry, S., Molday, L.L., and Molday, R.S. (2003). Functional interaction between the two halves of the photoreceptor-specific ATP binding cassette protein ABCR (ABCA4). Evidence for a non-exchangeable ADP in the first nucleotide binding domain. J. Biol. Chem. *278*, 39600–39608.

Aleksandrov, L., Aleksandrov, A.A., Chang, X.B., and Riordan, J.R. (2002). The First Nucleotide Binding Domain of Cystic Fibrosis Transmembrane Conductance Regulator Is a Site of Stable Nucleotide Interaction, whereas the Second Is a Site of Rapid Turnover. J. Biol. Chem. *277*, 15419–15425.

Aller, S.G., Yu, J., Ward, A., Weng, Y., Chittaboina, S., Zhuo, R., Harrell, P.M., Trinh, Y.T., Zhang, Q., Urbatsch, I.L., and Chang, G. (2009). Structure of P-glycoprotein reveals a molecular basis for poly-specific drug binding. Science *323*, 1718–1722.

Allikmets, R., Singh, N., Sun, H., Shroyer, N.F., Hutchinson, A., Chidambaram, A., Gerrard, B., Baird, L., Stauffer, D., Peiffer, A., et al. (1997a). A photoreceptor cell-specific ATP-binding transporter gene (ABCR) is mutated in recessive Stargardt macular dystrophy. Nat. Genet. *15*, 236–246.

Allikmets, R., Shroyer, N.F., Singh, N., Seddon, J.M., Lewis, R.A., Bernstein, P.S., Peiffer, A., Zabriskie, N.A., Li, Y., Hutchinson, A., et al. (1997b). Mutation of the Stargardt disease gene (ABCR) in age-related macular degeneration. Science *277*, 1805–1807.

Althoff, T., Mills, D.J., Popot, J.L., and Kühlbrandt, W. (2011). Arrangement of electron transport chain components in bovine mitochondrial supercomplex I1III2IV1. EMBO J. *30*, 4652–4664.

Beharry, S., Zhong, M., and Molday, R.S. (2004). N-retinylidene-phosphatidylethanolamine is the preferred retinoid substrate for the photoreceptor-specific ABC transporter ABCA4 (ABCR). J. Biol. Chem. *279*, 53972–53979.

Biswas-Fiss, E.E., Kurpad, D.S., Joshi, K., and Biswas, S.B. (2010). Interaction of extracellular domain 2 of the human retina-specific ATP-binding cassette transporter (ABCA4) with all-trans-retinal. J. Biol. Chem. *285*, 19372–19383.

Bungert, S., Molday, L.L., and Molday, R.S. (2001). Membrane topology of the ATP binding cassette transporter ABCR and its relationship to ABC1 and related ABCA transporters: identification of N-linked glycosylation sites. J. Biol. Chem. *276*, 23539–23546.

Eskandari, S., Wright, E.M., Kreman, M., Starace, D.M., and Zampighi, G.A. (1998). Structural analysis of cloned plasma membrane proteins by freeze-fracture electron microscopy. Proc. Natl. Acad. Sci. USA *95*, 11235–11240.

Fitzgerald, M.L., Morris, A.L., Rhee, J.S., Andersson, L.P., Mendez, A.J., and Freeman, M.W. (2002). Naturally occurring mutations in the largest extracellular loops of ABCA1 can disrupt its direct interaction with apolipoprotein A-I. J. Biol. Chem. *277*, 33178–33187.

George, A.M., and Jones, P.M. (2012). Perspectives on the structure-function of ABC transporters: the Switch and Constant Contact models. Prog. Biophys. Mol. Biol. *109*, 95–107.

Gohon, Y., Dahmane, T., Ruigrok, R.W., Schuck, P., Charvolin, D., Rappaport, F., Timmins, P., Engelman, D.M., Tribet, C., Popot, J.L., and Ebel, C. (2008). Bacteriorhodopsin/amphipol complexes: structural and functional properties. Biophys. J. *94*, 3523–3537.

Hamel, C.P. (2007). Cone rod dystrophies. Orphanet J. Rare Dis. *2*, 7.

Higgins, C.F. (1992). ABC transporters: from microorganisms to man. Annu. Rev. Cell Biol. *8*, 67–113.

Higgins, C.F., and Linton, K.J. (2004). The ATP switch model for ABC transporters. Nat. Struct. Mol. Biol. *11*, 918–926.

Hohl, M., Briand, C., Grütter, M.G., and Seeger, M.A. (2012). Crystal structure of a heterodimeric ABC transporter in its inward-facing conformation. Nat. Struct. Mol. Biol. *19*, 395–402.

Holland, I.B., and Blight, M.A. (1999). ABC-ATPases, adaptable energy generators fuelling transmembrane movement of a variety of molecules in organisms from bacteria to humans. J. Mol. Biol. *293*, 381–399.

Illing, M., Molday, L.L., and Molday, R.S. (1997). The 220-kDa rim protein of retinal rod outer segments is a member of the ABC transporter superfamily. J. Biol. Chem. *272*, 10303–10310.

Jones, P.M., and George, A.M. (2009). Opening of the ADP-bound active site in the ABC transporter ATPase dimer: evidence for a constant contact, alternating sites model for the catalytic cycle. Proteins *75*, 387–396.

Kos, V., and Ford, R.C. (2009). The ATP-binding cassette family: a structural perspective. Cell. Mol. Life Sci. *66*, 3111–3126.

Lee, J.Y., Urbatsch, I.L., Senior, A.E., and Wilkens, S. (2002). Projection structure of P-glycoprotein by electron microscopy. Evidence for a closed conformation of the nucleotide binding domains. J. Biol. Chem. *277*, 40125–40131.

Maeda, A., Maeda, T., Golczak, M., and Palczewski, K. (2008). Retinopathy in mice induced by disrupted all-trans-retinal clearance. J. Biol. Chem. *283*, 26684–26693.

Martínez-Mir, A., Paloma, E., Allikmets, R., Ayuso, C., del Rio, T., Dean, M., Vilageliu, L., Gonzàlez-Duarte, R., and Balcells, S. (1998). Retinitis pigmentosa caused by a homozygous mutation in the Stargardt disease gene ABCR. Nat. Genet. *18*, 11–12.

Mehmood, S., Domene, C., Forest, E., and Jault, J.M. (2012). Dynamics of a bacterial multidrug ABC transporter in the inward- and outward-facing conformations. Proc. Natl. Acad. Sci. USA *109*, 10832–10836.

Molday, L.L., Rabin, A.R., and Molday, R.S. (2000). ABCR expression in foveal cone photoreceptors and its role in Stargardt macular dystrophy. Nat. Genet. *25*, 257–258.

Nickell, S., Park, P.S., Baumeister, W., and Palczewski, K. (2007). Three-dimensional architecture of murine rod outer segments determined by cryoelectron tomography. J. Cell Biol. *177*, 917–925.

Papermaster, D.S., Schneider, B.G., Zorn, M.A., and Kraehenbuhl, J.P. (1978). Immunocytochemical localization of a large intrinsic membrane protein to the incisures and margins of frog rod outer segment disks. J. Cell Biol. *78*, 415–425.

Papermaster, D.S., Reilly, P., and Schneider, B.G. (1982). Cone lamellae and red and green rod outer segment disks contain a large intrinsic membrane protein on their margins: an ultrastructural immunocytochemical study of frog retinas. Vision Res. *22*, 1417–1428.

Peelman, F., Labeur, C., Vanloo, B., Roosbeek, S., Devaud, C., Duverger, N., Denèfle, P., Rosier, M., Vandekerckhove, J., and Rosseneu, M. (2003). Characterization of the ABCA transporter subfamily: identification of prokaryotic and eukaryotic members, phylogeny and topology. J. Mol. Biol. *325*, 259–274.

Piehler, A.P., Ozcürümez, M., and Kaminski, W.E. (2012). A-Subclass ATP-Binding Cassette Proteins in Brain Lipid Homeostasis and Neurodegeneration. Front. Psychiatry *3*, 17.

Popot, J.L., Althoff, T., Bagnard, D., Banères, J.L., Bazzacco, P., Billon-Denis, E., Catoire, L.J., Champeil, P., Charvolin, D., Cocco, M.J., et al. (2011). Amphipols from A to Z. Annu. Rev. Biophys. *40*, 379–408.

Quazi, F., Lenevich, S., and Molday, R.S. (2012). ABCA4 is an N-retinylidene-phosphatidylethanolamine and phosphatidylethanolamine importer. Nat. Commun. *3*, 925.

Radermacher, M., Wagenknecht, T., Verschoor, A., and Frank, J. (1987). Three-dimensional reconstruction from a single-exposure, random conical tilt series applied to the 50S ribosomal subunit of Escherichia coli. J. Microsc. *146*, 113–136.

Shaikh, T.R., Gao, H., Baxter, W.T., Asturias, F.J., Boisset, N., Leith, A., and Frank, J. (2008). SPIDER image processing for single-particle reconstruction of biological macromolecules from electron micrographs. Nat. Protoc. *3*, 1941–1974.

Sun, H., and Nathans, J. (1997). Stargardt's ABCR is localized to the disc membrane of retinal rod outer segments. Nat. Genet. *17*, 15–16.

Sun, H., Molday, R.S., and Nathans, J. (1999). Retinal stimulates ATP hydrolysis by purified and reconstituted ABCR, the photoreceptor-specific ATP-binding cassette transporter responsible for Stargardt disease. J. Biol. Chem. *274*, 8269–8281.

Tsybovsky, Y., Wang, B., Quazi, F., Molday, R.S., and Palczewski, K. (2011). Posttranslational modifications of the photoreceptor-specific ABC transporter ABCA4. Biochemistry *50*, 6855–6866.

Vasiliou, V., Vasiliou, K., and Nebert, D.W. (2009). Human ATP-binding cassette (ABC) transporter family. Hum. Genomics *3*, 281–290.

Ward, A., Reyes, C.L., Yu, J., Roth, C.B., and Chang, G. (2007). Flexibility in the ABC transporter MsbA: Alternating access with a twist. Proc. Natl. Acad. Sci. USA *104*, 19005–19010.

Weleber, R.G. (1994). Stargardt's macular dystrophy. Arch. Ophthalmol. *112*, 752–754.

Weng, J., Mata, N.L., Azarian, S.M., Tzekov, R.T., Birch, D.G., and Travis, G.H. (1999). Insights into the function of Rim protein in photoreceptors and etiology of Stargardt's disease from the phenotype in abcr knockout mice. Cell *98*, 13–23.

